Journal of Applied Fluid Mechanics, Vol. 18, No. 12, pp. 3018-3035, 2025.
Available online at www.jafmonline.net, ISSN 1735-3572, EISSN 1735-3645.
https://doi.org/10.47176/jafm.18.12.3611

Investigation of Heat Transfer and Entropy Generation in a Parabolic Trough Collector Receiver using Square Porous Media and Nanofluids

H. Diafi†, S. Djouimaa, D. Guerraiche and S. Noui

Applied Physic Energetic laboratory, (L.P.E.A) Department of Physics, Faculty of Matter Sciences
University of Batna 1, Batna 05000, Algeria

†*Corresponding Author Email: halla.diafi@univ-batna.dz*

ABSTRACT

The main problem with parabolic trough collector receivers is the focus of solar radiation on one side of the tube, resulting in a non-symmetric heat flux distribution on the absorber. This condition leads to non-uniform temperature, deterioration of the absorber tube, and a decline in efficiency. To improve the performance of PTC systems, it is crucial to enhance heat transfer and achieve temperature uniformity in the absorber tube. The objective of the numerical investigation is to examine a two-dimensional absorber tube that includes seven copper matrices of square porous media and investigate their combined effects on heat transfer and temperature uniformity. The basis fluid in this numerical simulation is Syltherm 800, which is used under laminar flow conditions to examine the effects of four physical parameters: variations in the Reynolds number (300, 500, 1000, and 1500), porosity levels (91% and 95%), types of nanoparticles (Al_2O_3, CuO, and Cu), and nanoparticle volume fractions (1%, 2%, and 3%). The results signify that the presence of nanofluids maximizes the enhancement of heat transfer, especially at a 3% concentration of Cu/Syltherm 800 nanofluids in a smooth tube. The novel configuration significantly enhances heat transfer, offers a more homogeneous temperature, and reduces thermal energy losses by minimizing entropy generation, which makes the system more sustainable for long-term thermal applications. Reducing porosity from 95% to 91% in novel configurations improved heat transfer and thermal homogeneity but increased the coefficient of friction.

Article History

Received April 17, 2025
Revised June 29, 2025
Accepted July 30, 2025
Available online October 6, 2025

Keywords:

Porous media
Nanofluid
Laminar flow
Nusselt number
Entropy generation

1. INTRODUCTION

The latest development in solar energy technique is the parabolic trough collector (PTC), which is a popular type of concentrating solar power. Essentially, the collector captures the solar radiation in a single-axis focal parabolic mirror, which is reflected into the receiver tube. The receiver tube contains a working fluid, such as water, oil, or gas, which flows out and transmits heat to a heat exchanger that turns water into steam and operates a steam turbine to generate electrical power. The challenge arises when solar radiation is concentrated on one side of the tube while it is normal on the other. They create a non-symmetric heat flux distribution on the receiver tube, which causes high-temperature gradients and peaks. This situation can lead to the deterioration of parabolic trough collectors (PTCs), heat loss, and damage to the absorber tube (Jamal-Abad et al., 2018).

Several strategies have been proposed to resolve these problems and improve the performance of PTC. These include changing the shape of the absorber tube by adding fins, ribs, or a porous medium As well as altering the physical characteristics of the working fluid through the addition of nanoparticles, as this method is considered the most widely adopted recently in several fields (Guerraiche et al., 2022; Sheikholeslami & Khalili, 2025; Sheikholeslami et al., 2025; Naaim et al., 2025), or altering the shape of the absorber tube while also adding nanoparticles (Chakraborty & Nath, 2024a, b). While these strategies have shown promising results in enhancing PTC performance, further improvements are still necessary.

Heat transfer in porous media is a prevalent technique due to its ease of utilization in industrial applications and its demonstrated ability to improve thermal efficiency. Their efficiency improves since the solid parts

NOMENCLATURE

Be	Bejan number	*in*	inlet
q'	heat flux density	*nf*	nanofluid
ε	porosity	*out*	outlet
s	solid	PTSC	Parabolic Trough Solar Collector
v	velocity	PTR	Parabolic Trough receiver
φ	volume fraction	PM	Porous Media
Subscripts		0	tube with only the basic fluid
f	fluid		

of the porous media augment the thermal conductivity of the fluid (Esapour et al., 2018; Abbasi et al., 2020).

This paper focuses on research that uses porous media and nanofluids in a receiver tube to increase PTC efficiency. A plethora of conventional porous media inserts have been used to enhance parabolic trough collectors, including the porous disc, porous fin, metal foam, and packed bed.

Many researchers have focused their study on using porous discs to boost the performance of the parabolic trough receiver tube, including Ravi Kumar and Reddy (2012), who studied the impact of varied placement of a porous disc in a receiver tube on the performance of a parabolic trough collector (at the top, at the bottom, slope upward, slope downward, and alternate porous disc) and the influence of working fluid (water and Therminol Oil 55). The results revealed an ideal enhanced heat transfer rate for the pattern of porous discs at the bottom with water and at the slope downward with Therminol Oil 55 in an experimental analysis of a PTC with six receivers composed of different porous discs. Bozorg et al. (2020) studied the use of a circular porous medium within a parabolic trough collector, added it to the working fluid Al_2O_3/synthetic, and numerically simulated the flow in a turbulent regime for Reynolds numbers between 5×10^4 and 60×10^4. Researchers found that using porous structures and nanoparticles simultaneously increases heat transfer coefficients, pressure, thermal efficiencies, and overall efficiencies.

Otherwise, the researchers also used porous fins. For example, Peng et al. (2021) investigate the effects of a novel insertion of porous fins into absorber tubes, specifically semi-annular and fin-shaped metal foam (triangle, rectangle, and trapezoid). They found that adding metal foam significantly increases the Nusselt number, friction factor, PEC, and total entropy generation reduction. They also noticed that the triangular shape presents the optimal enhanced heat transfer. Panja et al. (2024) enhanced the thermal performance of PTSC by modifying the absorber tube with the insertion of porous obstacles containing CuO and Al_2O_3 nanofluids at varying volume concentrations from 3% to 7%. This approach aims to optimize the system's heat transfer capabilities. Laminar flow conditions for Reynolds numbers between 500 and 2000 and a constant heat flux of 800 W/m² are used for the simulations. They concluded that incorporating porous obstacles and utilizing nanofluids presents a promising method to enhance the thermo-hydraulic performance of PTSC, providing valuable insights for improving solar collector efficiency. They recorded the maximum thermal performance factors for CuO nanofluids.

Within the previous literature, several numerical and experimental studies have been adopted for enhancing the efficacy of parabolic trough collectors with indicated metal foam. For example, Wang et al. (2013) employed numerical simulations to explore the impact of incorporating metal foams in a PTC receiver tube on heat transfer. The arrangement (bottom/top), height (H), and porosity (ε) of the metal foams impact the flow resistance. Jamal-Abad et al. (2017) used copper metal foams inner a tube absorber with 90% porosity. The experiment results illustrate that including metal foam in the absorber improves collection efficiency, and the total loss factor of the solar collector drops by 40%. Tayebi et al. (2019) examined numerically the effect of 64-cm copper metal foams, Al_2O_3, and TiO_2/water nanofluids on a three-dimensional direct absorption parabolic trough collector with (0.1, 0.2, and 0.3) volume fractions. Their results indicate a peak efficiency for 3% volume fractions of TiO_2/water. Valizade et al. (2020) performed an experimental examination on heat transfer improvements in an absorption tube employing metal foam with a porosity of 0.90. They evaluated three situations (without porous media, with a semi-porous medium, and with a completely porous medium). The study found that the temperature difference decreased by 12.2°C in the tube without porous media, 8.8°C in the tube with semi-porous media, and 3.3°C in the tube with completely porous media. The maximum thermal efficiency, 60%, was reached in the totally porous medium. Heyhat et al. (2020) led experimental research on the outcomes of using different volume concentrations of CuO/water nanofluids, metal foam with 95% porosity, and their mixture on the thermal efficiency of PTSC. The results validated the excellent efficacy of metal foam and nanofluid, particularly at lower flow rates. Peng et al. (2020) presented a simulation of heat transfer in a PTR tube partially filled with gradient metal foam (GMF). They study their impacts on Nusselt number, entropy generation rate, PEC, etc. They conclude that GFM improved thermal-hydraulic and thermodynamic efficiency. Hooshmand et al. (2021) provided an experimental study of the consequences of using metal foam at two different pores (0.95 and 0.98) on the direct absorber solar collector with SiC/water nanofluid at three different concentrations. The results suggest that the foam insertion optimizes all efficiency. Esmaeili et al. (2023) led an experimental study to determine the impact of placing metal foam in

three places on the absorber tube's performance: a periodic foam, filling the entry half, and the exit half. The results of laminar flow showed that the absorber tube with periodic foam performed the best.

In this area of research, other studies used the porous medium as a way to improve the PTSC absorber tube and have proven their efficiency in enhancing thermal performance; for example, Hatami et al. (2018) placed a porous media annulus inside a two-dimensional absorber tube and suspended nanofluids. They studied several physical variables: nanoparticle types, volume fraction, porosity, and Reynolds number. They confirmed their findings that the maximum Nusselt numbers occur when the volume fraction is 8% and Rayleigh at the high value. Also, Cu nanoparticles show the greatest increase in the number of Nusselt compared to other used particles. Das et al. (2021) record a numerical examination of heat transfer in a receiver tube for several porous media: different heights and different geometrical forms (the bottom half is filled with porous medium, and the modified bottom half is filled to a corrugated shape). They found that heat transfer enhancement is excellent in turbulent and transitional flow regimes. Also, the modified bottom half demonstrates boost heat transfer. The inclusion of nanoparticles improves thermal efficiency by raising the concentration of Cu nanoparticles.

Recently, the backed bed has been used to raise the absorber tube efficiency. For example, Wei et al. (2024) introduced the unique PTSR-R, which is a receiver tube separated into two channels of flow by a central vertical separator and another by a central horizontal separator. This tube is filled with catalyst-particle-packed beds. Horizontal separation was found to lower significantly the highest temperature of PTSR-R, improving the methanol conversion rate's upper limit by 7.15%. The vertical separation is capable of effectively enhancing temperature uniformity and reaction performance.

According to the above literature review, many categories of porous media, such as porous discs, metal foam, porous fins, packed beds, etc., were proposed to improve PTC systems. However, it is clear that more research needs to be done to study the effect of the porous medium in the absorber tube.

The previous literature suggests that applying porous media or combining it with nanofluids can assist in boosting the performance of parabolic trough collectors (PTCs). However, previous studies have not adequately investigated the specific impact of porous media on temperature uniformity, and only a limited number have examined thermodynamic aspects such as entropy generation minimization in parabolic trough collectors, including (Mwesigye et al., 2013; Ekiciler et al., 2023), have investigated entropy generation in parabolic trough collectors. This factor is critical for optimizing energy systems by determining the irreversibility of system components. Furthermore, although porous media are commonly used in absorber tubes, no study to date has focused on the role of square-structured porous media in PTC receivers despite their potential to improve flow mixing and enhance thermal performance.

Table 1 Parabolic Trough Collector: Specific Dimensions

Inner diameter D_{ri} (mm)	22
Outer diameter D_{ro}(mm)	26
The Length for absorber tube L (mm)	1400
Width of collector W (mm)	700
The concentration ratio $C = A_a/A_r$	8.56

Table 2 Porous Media Geometry

parameter	value	
Material	Copper	
Porosity ε	0.91	0.95
Distance H (mm)	3	4
Obstacle Diameter D (mm)	0.89	

This research proposes a numerical examination of a novel configuration of the absorber tube of a parabolic trough collector (PTC), combining the application of square porous media with different nanofluids to increase thermal performance and homogenize the temperature. The porous media comprises groups of square solids, which we refer to as the matrix. This novel absorber tube contains seven equidistant matrices with a 100 mm length and 18 mm width. The porous medium consists of a square solid positioned in an alternating arrangement. The absorber tube is exposed to concentrated solar flux reflected by the parabolic reflector. This research involves various case studies, including the type of nanofluids, their volume fraction, porous media porosity, and Reynolds number. To assess the influence of these factors on the Nusselt number, friction coefficient, entropy generation, and Bejan number.

2. PHYSICAL MODEL

The prototype parabolic trough absorber tube relied on in this study was experimentally adopted by (Valizade et al., 2020). The specified dimensions of the receiver are detailed in Table 1. where the length is 1400 mm, the internal diameter is D_{ri} = 22 mm, the thickness is 4 mm, and the width of the collector is W = 700 mm.

The objective of this work is to enhance heat transfer and achieve greater uniformity in temperature distribution on the surface of the tube. For this aim, a novel model was proposed that incorporates the addition of seven sections (matrices) of a porous medium, as illustrated in Fig. 1. The porous medium was created by generating a periodic structure of staggered arrangements of square solid obstacles. Each group of porous media is referred to as a 'matrix'; these seven matrices are equal, and each one is 100 mm long and 18 mm high. For a more precise representation, a zoomed-in matrix geometry of the porous medium is illustrated in Fig. 1b. Also, Table 2 indicates the dimensions and diameter of the pores and the possibility of controlling and monitoring the porosity depending on the distance between the solid parts and the diameter of the pores, where the pore diameter is fixed at d = 0.89 mm. For h = 3 mm, the porosity is 91%, while for h = 4 mm, the porosity is 95%, according to the following

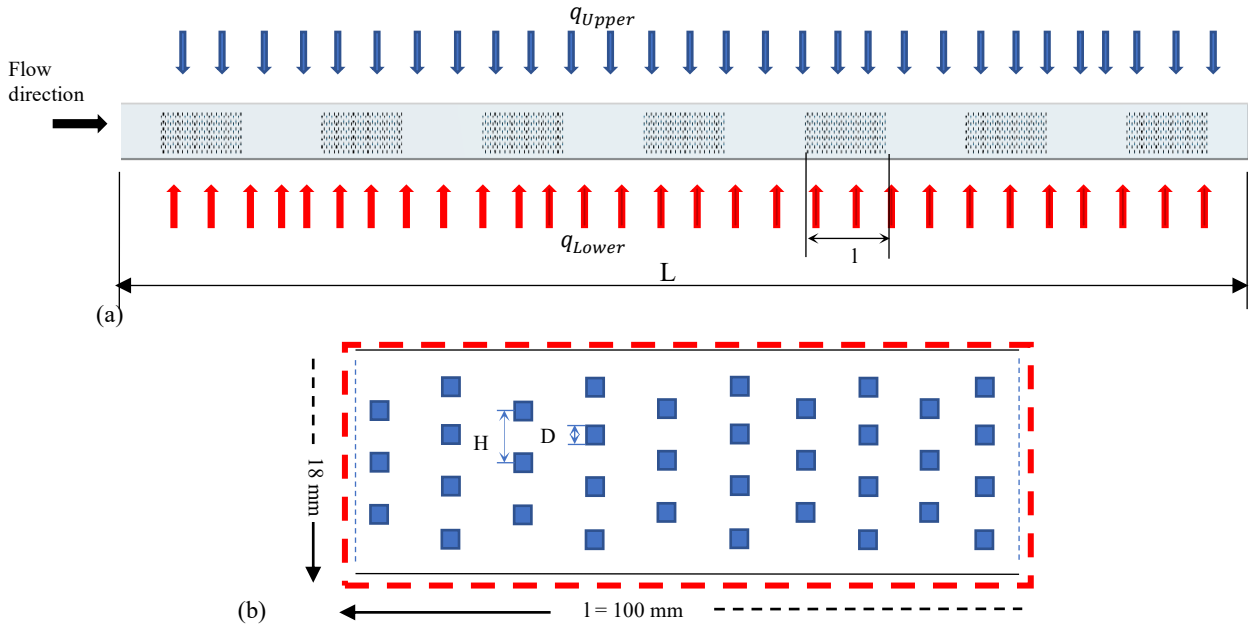

Fig. 1 a) Schematic of absorber tube with seven matrices of square porous media and b) a zoomed-in porous matrix geometry

relationship (Kuwahara et al., 2001a):

$$\varepsilon = 1 - \left({}^{D}/_{H}\right)^{2} \quad (1)$$

Solar radiation is directly on the top half of the tube q_{Upper}, and concentrates on the bottom q_{Lower}, where the ratio of concentration is defined as: $C = A_a/A_r$. The areas of the collector and the absorber tube are specified as A_a =W. L and $A_r = \pi . D_{ro}.L$, respectively.

3. GOVERNING EQUATIONS:

The governing equations used in this study for laminar and steady-state flow through a saturated porous medium are proposed by (Chen et al., 2016) for continuity and momentum equations and by (Xu et al., 2011) for the energy equation. These equations are as follows:

Continuity equation:

$$\nabla.\left(\rho_f.\vec{V}\right) = 0 \quad (2)$$

When $\vec{V}$ denotes the superficial velocity and ρ_f is the fluid density.

Momentum equation:

$$\frac{1}{\varepsilon}\nabla.\left(\rho_f \frac{\vec{V}.\vec{V}}{\varepsilon}\right) = -\nabla P + \nabla.\left(\frac{\mu_f}{\varepsilon}\nabla\vec{V}\right) + \vec{F} \quad (3)$$

The variables in the equation are as follows: P represents the pressure of the fluid, μ_f: the fluid dynamic viscosity, ε: the porosity, $\vec{F}$: indicates the momentum source, which determines the pressure drop caused by porous media.

Energy equation (Xu et al., 2011):

For the solid phase:

$$0 = \nabla.\left(\frac{1}{3}(1-\varepsilon)\lambda_s.\nabla T_s\right) + \alpha_{sf}h_{sf}\left(T_f - T_s\right) \quad (4)$$

For the fluid phase:

$$\nabla.\left(\rho_f c_p T_f \vec{V}\right) = \nabla.\left(\varepsilon\lambda_f.\nabla T_f\right) - \alpha_{sf}h_{sf}\left(T_f - T_s\right) \quad (5)$$

The fluid and solid temperatures are denoted as T_f and Ts, respectively. C_p, the specific heat of the fluid. Thermal conductivity for the solid and fluid phases are $\lambda_{\_s}$ and $\lambda_{\_f}$ respectively.

h_{sf} is the thermal conductivity coefficient among the porous matrix and the fluid (W/m^2.K), and α_{sf} is the specific surface area per unit volume in (m^{-1}) $\alpha_{sf} = 6(1-\varepsilon)/D$

4. MATHEMATICAL FORMULATION:

In addition to the conservation equations, we present the following:

4.1 Basic Thermal and Hydraulic Analysis:

The presented equations (6-10) describe and outline the parameters to be used to characterize the phenomena in this study.

The heat transfer rate (W):

$$Q_u = \dot{m}C_p(T_{out} - T_{in}) \quad (6)$$

The Reynolds number:

$$Re = \frac{4.\dot{m}}{\pi.D_{ri}.\mu} \quad (7)$$

The heat transfer factor (W/m^2.K):

$$h = \frac{\varphi_u}{(\pi.D_{ri}.L)(T_r - T_{fm})} \quad (8)$$

The mean Nusselt number:

$$Nu = \frac{h.D_{ri}}{\lambda} \quad (9)$$

The friction factor (Shah & London, 1978):

$$f = \frac{2\tau_w}{\rho v^2} \quad (10)$$

Where ṁ, T_r, T_{fm}, τ_w, v, and ρ represents the mass flow (Kg/s), Temperature in the inner of absorber tube (K),

The average working fluid temperature (K), the wall shear stress (Pa), velocity of the fluid, and the fluid density (Kg/m^3).

4.2 Other Equation Used in the Correlations

The correlation of (Wakao, N., & Kagei, 1982; Kuwahara et al., 2001b) given for laminar flow is used to validate the numerical simulations:

$$Nu = 1 + \frac{4(1-\varepsilon)}{\varepsilon} + \frac{1}{2}(1-\varepsilon)^{1/2} Re_d^{0.6} Pr^{1/3} \quad (11)$$

Re_d, P_r present the unitless number of Reynolds and Prandtl, where Re_d is based on the diameter of the pores ($Re_d = (1-\varepsilon)^{1/2}Re$).

4.3 Performance Evaluation Criteria (PEC) (Webb, 1981):

The PEC is a critical parameter for informing and assessing how much thermal and hydraulic performance improves with any enhancement technology. This parameter is expressed as:

$$PEC = \frac{Nu/Nu_0}{f/f_0^{1/3}} \quad (12)$$

where Nu_0 and f_0 represent the values of the Nusselt number and friction factor for a smooth tube without any changes.

4.4 Entropy Generation and Bejan Number (Bejan, 1996):

Enhancing heat transfer while minimizing thermodynamic irreversibility is a crucial challenge when designing efficient solar thermal systems. The second principle of thermodynamics offers a valuable framework for evaluating this exchange through entropy generation analysis. Minimizing entropy generation is crucial for achieving an optimal absorber tube design, which enhances heat transfer and reduces energy dissipation. This leads to more efficient and sustainable parabolic trough collector systems. The following equation summaries the total entropy generation rate per unit tube length (W/m.K), where is composed of two parts: one caused by heat transfer ($\dot{S}'_{gen,h}$) and the other caused by fluid friction ($\dot{S}'_{gen,f}$).

$$\dot{S}'_{gen} = \dot{S}'_{gen,h} + \dot{S}'_{gen,f} \quad (13)$$

Where, the entropy generation by heat transfer per unit length in the eq (14) results from temperature differences between the absorber tube wall to a fluid (W/m.K).

$$\dot{S}'_{gen,h} = \frac{q'^2}{\pi\lambda T_{fm}^2 Nu} \quad (14)$$

And the entropy generation by fluid friction per unit length in the eq (15) results due to fluid viscosity, internal friction arises between the fluid and the tube wall (W/m.K).

$$\dot{S}'_{gen,f} = \frac{32\dot{m}^3 f}{\pi^2\rho^2 T_{fm} D_{ri}^5} \quad (15)$$

Entropy generation in detailed form:

$$\dot{S}'_{gen} = \frac{q'^2}{\pi\lambda T_{fm}^2 Nu} + \frac{32\dot{m}^3 f}{\pi^2\rho^2 T_{fm} D_{ri}^5} \quad (16)$$

The Bejan number is a dimensionless value determines the quantity of heat transfer irreversibility that results in total entropy generation; it is given by Eq. (16). When the Bejan number approaches zero (0), fluid friction irreversibilities dominate; conversely, when it approaches one (1), heat transfer irreversibilities become predominant. This parameter helps identify which physical mechanism is primarily responsible for entropy generation in the system and is useful for optimizing energy efficiency.

$$Be = \frac{\dot{S}'_{gen,h}}{\dot{S}'_{gen}} \quad (17)$$

4.5 Thermophysical Properties and Nanofluids

The working fluid used in the receiver is Syltherm 800; its properties change with temperature, as shown in Table 3 (Delgado-Torres & García-Rodríguez, 2007). Copper is the material used for the tube, with has the following characteristics: density of 8978 (kg/m^3), specific heat capacity of 381(J/kg. k), and thermal conductivity of 387.1 (W/m.k), and the nanoparticles properties and correlations of nanofluids are used in Tables 4 and 5, respectively.

5. GRID GENERATION AND INDEPENDENCE CHECKING

To check the reliability and accuracy of the numerical solution, a structured quadratic was generated for the smooth absorber and both novel configurations, with local refinement in the inlet, outlet, near the walls, and around the square parts to capture boundary layer gradients and local flow physics in those zones. Several refinements reveal that the mesh element has no impact on the solution's results for different cell numbers. The grid is obtained using the paving scheme. Figure 2.a shows the mesh for **ε** = 0.91 and 1318857 elements.

The verification of the independence mesh includes tracing the static temperature along the tube at y = 0.01 m; the three configurations yield the following independence grid: The smooth tube is represented by Fig. 2.b, while the tube with matrices and varying porosities is represented by ε = 95% in Fig. 2.c and 91% in Fig. 2.d, respectively. It is noted in their figures that the numerical solution is not affected by the change in static temperature along the length of the tube.

To further verify the independence mesh, Table 6 shows the relative errors of the Nusselt and friction factor number outputs for all configurations. This verification was conducted at a Reynolds number of 500 and an initial temperature of 400 K. The relative error is calculated using the relationship below (Shah & London, 1978):

Table 3 Thermophysical parameters

Paramètres	Fluid (Syltherm 800)
Density (kg/m^3)	$\rho = -6.06165\times10^{-4}.T^2 - 0.415349.T + 1105.7$
Specific heat capacity (J/kg. k)	$C_P = 1.\ 708.T + 1107.798$
Thermal conductivity (W/m.k)	$\lambda = -5.75349\times10^{-10}.T^2 - 1.8752\times10^{-4}T + 0.19002$
Viscosity (µPa.s)	$\mu = 6.67233\times10^{-7}.\ T^4 - 1.566.\ \times10^{-3}T^3 + 1.3882.T^2 - 554.127T + 8.4866\times10^4$

Table 4 Nanoparticules properties (Büyük Öğüt, 2009)

Nanoparticles	ρ_s (kg/m^3)	K_s(W/m.k)	$C_{P\,s}$ (J/kg. k)
Al_2O_3	3970	40	765
CuO	6500	20	535.6
Cu	8933	400	385

Table 5 Correlations of the thermophysical properties used in the nanofluid

Properties	Correlation of mono-nanofluid equations
Density (Pak & Cho, 1998)	$\rho_{nf} = (1-\varphi)\rho_f + \varphi\rho_s$
Specific thermal capacity (Tayebi & Chamkha, 2016)	$(\rho C_p)_{nf} = \varphi(\rho C_p)_s + (1-\varphi)(\rho C_p)_f$
Dynamic viscosity (Brinkman, 1952)	$\mu_{nf} = \dfrac{\mu_f}{(1-\varphi)^{2.5}}$
Thermal conductivity (Maxwell, 1881)	$\dfrac{k_{nf}}{k_f} = \dfrac{2k_f + k_s + 2\varphi(k_s - k_f)}{2k_f + k_s - \varphi(k_s - k_f)}$

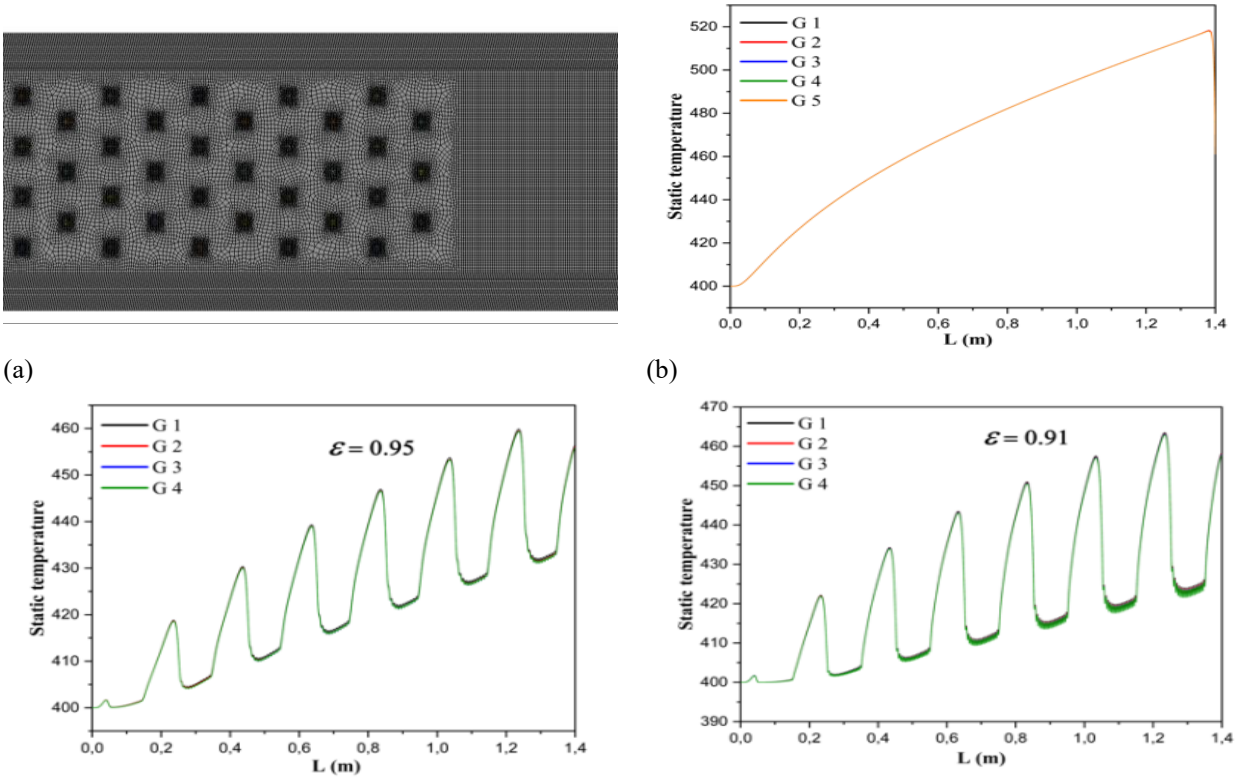

Fig. 2 Computational and Independence Grids

$$E(\%) = \frac{|e_2 - e_1|}{e_1} \times 100 \qquad (18)$$

Where (e) represents any parameter; in this study, it represents the Nusselt number and friction factor. e_1 represents the values reached, representing the best mesh accuracy, while e_2 represents the values reached at the lowest mesh accuracy. Based on the calculated relative error in Table 6 and the computational time taken, the results were accepted for 3421280 elements of the smooth tube, 1446873 elements of the tube at 95% porosity, and 2920927 elements of the tube at 91% porosity, with a maximum error of 0.24% between the three cases.

Table 6 Mesh Independence Check

Geometry	Grid	Elements	Nu	*f*	% Nu	% *f*
Smooth tube	G1	1748096	8.47451	0.02415	-	-
	G2	2244224	8.50999	0.02416	0.41866	0.04141
	G3	2801952	8.54079	0.02417	0.36192	0.04139
	G4	3421280	8.56014	0.02418	0.22656	0.04137
	G5	4102208	8.56976	0.02419	0.11238	0.04136
Tube with porous media (95%)	G1	638371	11.14332	0.11657	-	-
	G2	924787	11.09093	0.11690	0.47015	0.28309
	G3	1225427	11.0546	0.11712	0.32756	0.18820
	G4	1446873	11.03827	0.11711	0.14772	0.00854
Tube with porous media (91%)	G1	1318857	13.0275	0.19661	-	-
	G2	1837810	12.95729	0.19727	0.53894	0.33569
	G3	2315966	12.92924	0.19804	0.21648	0.39033
	G4	2920927	12.89811	0.19851	0.24077	0.23733

6. NUMERICAL METHOD

In this simulation the numerical solutions using the finite volume method in ANSYS 19.1 software. The numerical solution procedure adopts the coupled algorithm for pressure–velocity and a second-order upwind scheme to discretize all the studied cases. The convergence criterion for all residuals is 10^{-6}.

7. BOUNDARY CONDITIONS:

The ensuing boundary conditions are implemented in the absorber tube as:

- Inlet: the flow input is at a constant temperature of 400 K, the imposed uniform and constant velocity is. $u_x = u_{in}$, $u_y = 0$
- Outlet: the outflow (conservation of energy and mass flow).
- The coupled condition is used at the interface fluid and Solid Square.
- Wall of receiver: The unique configuration of the reflector determines non-uniform heat flow as indicated in Fig.1.

a) The upper half of the receiver is exposed to:

$$q_{upper} = \varphi_{solaire} \times \tau_{glass} \times \alpha_{absorber} = 912\ w/m^2$$

b) The lower half of the receiver is exposed to:

$$q_{lower} = \varphi_{solaire} \times \tau_{glass} \times \alpha_{absorber} \times C = 7815.7\ w/m^2$$

The transmissivity for the cover is represented by τ_{glass}, the absorber tube's absorptivity by ($\alpha_{absorber}$), incident solar radiation (w/m^2) by (φ_{solar}), and the concentration ratios of C, 0.96, 0.95, 1000, and 8.56, respectively.

8. RESULTS AND DISCUSSION

A numerical analysis of a receiver tube in a PTC is performed in a two-dimensional configuration under steady-state conditions. A direct and concentrated heat flux is applied to the upper and lower surfaces of the tube, inducing a temperature gradient and an asymmetric heat distribution. This asymmetry directly affects entropy generation and the Bejan number, influencing the overall heat transfer process.

To improve thermal efficiency and avoid the non-homogeneity of temperature, the study investigates the usage of nanoparticles (Al_2O_3, CuO, and Cu) at volume fractions of 1%, 2%, and 3%. The enhanced thermal conductivity can help to reduce temperature gradients and limit entropy generation.

Another method of addressing non-symmetric heat flux is the addition of porous media inside the tube. Two levels of porosity (91% and 95%) were tested to evaluate their potential to redistribute heat more evenly while lowering entropy generation.

Results are presented for key parameters, especially the Nusselt number, entropy generation, Bejan number, and performance evaluation criteria. The study was executed at an inlet temperature of 400 K and Reynolds numbers of 300, 500, 1000, and 1500, providing a comprehensive assessment of the effect of heat flux non-uniformity and the effectiveness of the proposed solutions.

8.1 Validation of Results

To evaluate the reliability and accuracy of the simulation's results, the numerical data for the Nusselt number in a porous medium (ε = 0.91) were compared with Wakao and Kagei, (1982) correlation as obtained in equation (11). The comparison in Fig. 3 shows that the Nusselt number is closest to the validity correlation, especially for Reynolds larger than or equal to 1000. This slight deviation confirms the quality and substantiate the credibility of the computational model used in our study, which aligns with reference data validation.

8.2 Flow Structure

The flow structure has a forceful effect on the convective heat transfer performance. It is essential to have a detailed analysis of the velocity and temperature fields.

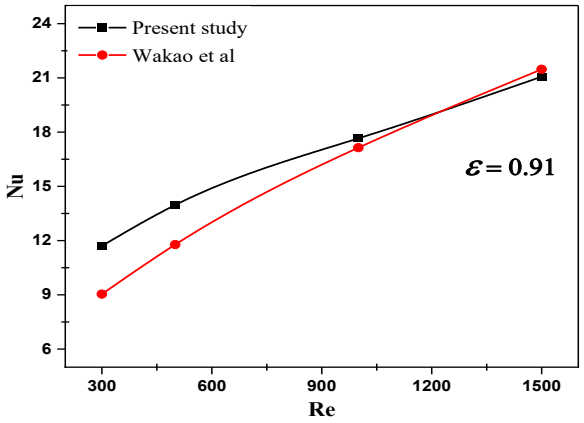

Fig. 3 Validation of Nusselt number for tube with porous media

8.2.1 Velocity field

Figure 4 illustrates the velocity and temperature contours of the flow field in the absorber tube with Re = 1000 and porous inserts. In Fig. 4.a. Porous media generates vortexes around the elements of the square matrix. The appearance of these vortexes and the increase in velocity near the wall of the absorber tube create a perturbation in the boundary layer, allowing the fluid to mix within the absorber tube. Additionally, the velocity rises when porosity is reduced. This is according to the law of Mass Conservation; the decrease in the area available for fluid flow due to decreased porosity requires an increase in flow velocity to retain a constant mass flow. The increase in fluid velocity near the walls of the porous tube is extremely beneficial for rapid heat transfer, thereby facilitating fluid mixing.

8.2.2 Temperature Field

One of the important characteristics of PTCs is the absorber tube temperature. To study this, the fluid temperature distribution was considered under the same conditions presented above. According to Fig. 4b, it is evident that a high-temperature gradient exists among the top and bottom sections of the absorber tube, resulting in considerable thermal strain and reducing the useful life of the PTR. The presence of the porous media reduces the temperature peak on the concentrated side of the tube. In addition, as demonstrated in Fig. 5 for Y = 1.1 mm, the temperature along the absorber tube walls is further raised by the addition of a 3% volume fraction of Cu nanoparticles. On the other hand, the novel tube disturbs the thermal layer in the porous media zones, leading to temperature fluctuations and decreases. This variation arises as a result of the solid-fluid interaction, in which the solid components absorb the fluid's heat since their temperature is lower than the fluid's. Hence, combining the porous medium and nanofluid creation makes the fluid more homogeneous and improves thermal transfer.

8.3 Nusselt Number and Friction Factor

8.3.1 The Effect of Semi-Porous Media Without Nanofluids

Figure 6. a show how the Nusselt number changes with the Reynolds number in the absence of nanofluids. It is indicated that the Nusselt number increases with the rise of the Reynolds number; this enhancement is more

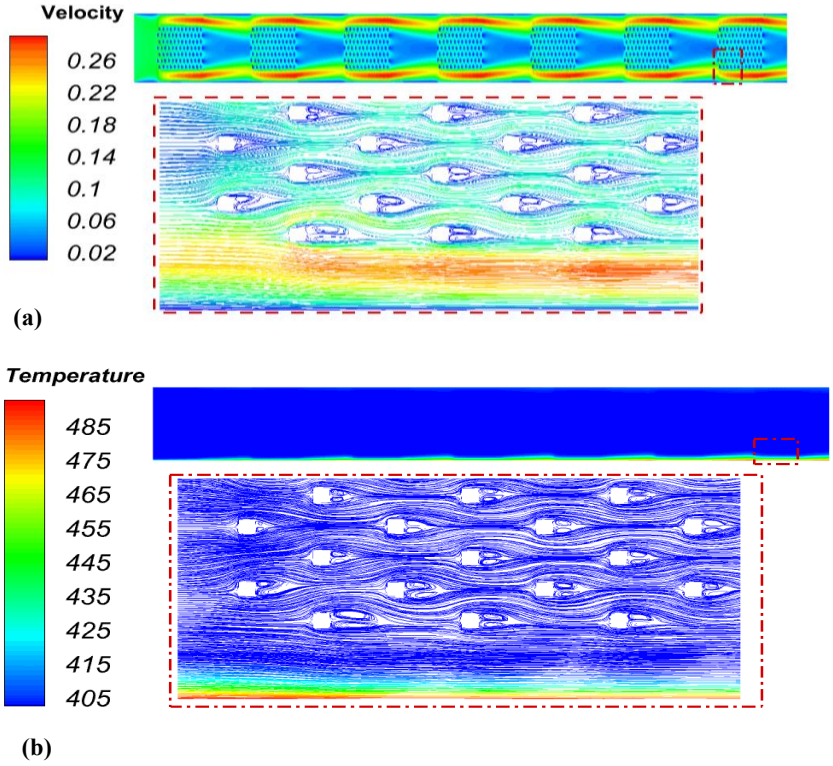

Fig. 4 a) Velocity contour and b) Temperature contour for a tube with porous media ε=95%

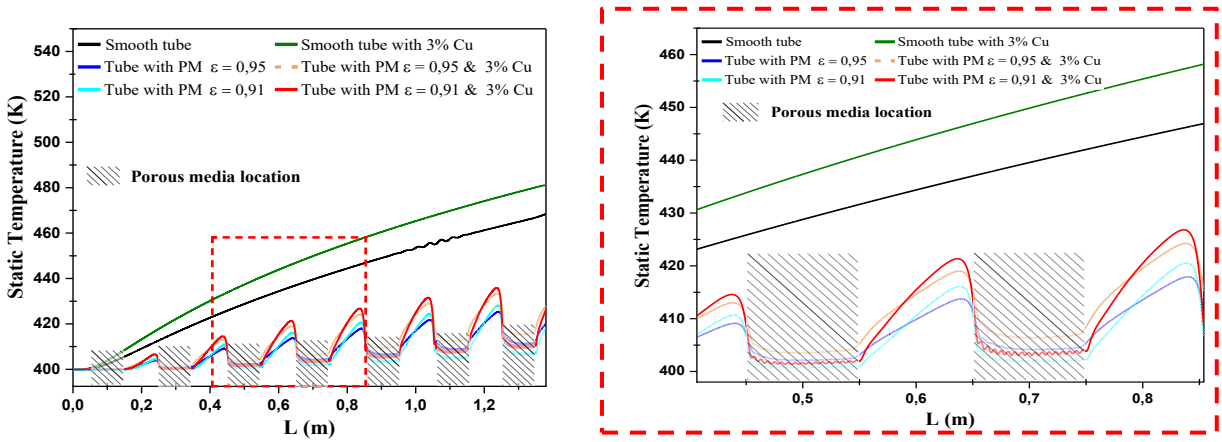

Fig. 5 Temperature near the lower thermal boundary layer of the tube (Y = 1.1 mm).

noticeable in the presence of porous media and when the porosity decreases. This augmentation is because of an increase in thermal conductivity and improved local convective mixing within the porous media, which significantly improves heat transfer. For example, at Re = 1000, the smooth tube yields a Nusselt number evaluated at about 11.11. When inserting the matrices with ε = 95%, the Nusselt number goes up to 16.90, which gives an improvement of 52.1%. The porous medium allows more thermal mixing and energy exchange between the fluid layers. As the porosity decreases to ε = 91%, the Nusselt number rises to 17.66. This value represents a 58.9% enhancement. Reduced porosity increases the solid fraction and reduces void space, thereby enhancing the effective thermal conductivity and promoting the interaction between the fluid and solid parts, thus increasing the heat transfer mechanism.

Figure 6.b shows that the friction factor increases dramatically when semi-porous media are introduced and continues to rise as porosity decreases due to the increase in contact surface area, which leads to obstruction of flow, leading to increased pressure loss. For example, at Re = 300 and ε = 91%, the friction factor achieves a high value of 0.2949, compared to 0.033 in the smooth tube. This substantial increase reflects the higher flow resistance introduced by the porous inserts.

8.3.2 Effects of Nanofluids without Semi-Porous Media

The examination of how the Nusselt number varies with the Reynolds number for three different nanoparticles (Al_2O_3, CuO, and Cu) at volume fractions of 1%, 2%, and 3% and compared to a smooth tube without nanofluid is given in Fig. 7. a. The results demonstrate that the Nusselt number increases with the Reynolds number and rises in the nanoparticle volume fraction. Among the nanofluids, Cu/Syltherm 800 consistently provides the best heat transfer. This enhancement is attributed to the higher thermal conductivity of Cu compared to Al_2O_3 and CuO. In addition, the effect is more pronounced at high Reynolds numbers, where convection forces dominate. Table 7 presents the Nusselt number data for the smooth tube. According to Fig 7. a and the data of Table 7, it can demonstrate as an example improvement for uses of Cu/syltherm 800 of [3.29% to 8.37%] for 1% volume

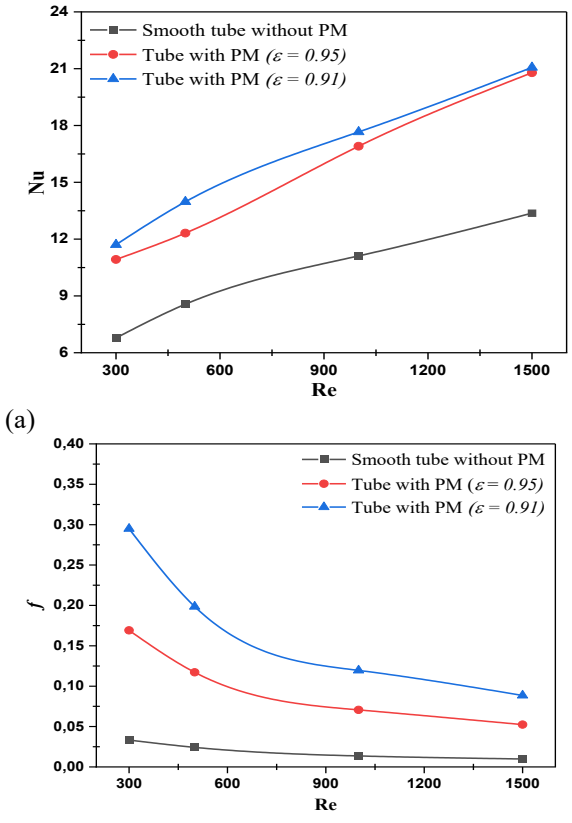

Fig. 6 Effect of different porosity of Porous media compared with smooth tube: a) Nusselt number, b) friction factor

fractions, [11.89% to 16.83%] for 2%, and [20.07% to 25.38%] for 3% when compared to the smooth tube. Notably, Cu/Syltherm 800 at 2% outperforms 3% Al_2O_3/Syltherm 800, achieving gains between [10.51% and 14.85%].

Figure 7.b. illustrates the influence of the friction factor as a function of three variables: the Reynolds number, the different nanofluids, and volume fractions. Generally, the friction factor in the base fluid increases with increasing Reynolds values. However, the inclusion of nanoparticles results in a noticeable increase in the friction factor; the extent of this increase depends on the

Table 7 Data of Nusselt number for a smooth tube, Tube with porous media ε = 95%, and Tube with porous media ε= 91%

Smooth tube-Nusselt number-											
Volume fraction		0%	1%			2%			3%		
Type of NF		----	Al_2O_3	CuO	Cu	Al_2O_3	CuO	Cu	Al_2O_3	CuO	Cu
Re	300	6.777	6.846	6.946	6.999	7.172	7.320	7.582	7.508	7.809	8.139
	500	8.560	8.636	8.762	8.906	9.040	9.303	9.588	9.461	9.855	10.279
	1000	11.113	11.639	11.828	12.034	12.195	12.366	12.978	12.766	13.329	13.934
	1500	13.373	13.839	14.075	14.209	14.388	14.846	15.341	15.065	16.742	16.487
Tube with porous media ε = 95% - Nusselt number-											
Re	300	10.926	11.175	11.246	11.343	11.647	11.821	12.012	12.135	12.396	12.664
	500	12.314	14.013	14.114	14.264	14.557	14.805	15.092	15.130	15.507	15.931
	1000	16.902	18.894	19.079	19.319	19.626	19.987	20.382	20.364	20.910	21.541
	1500	20.785	22.937	23.250	23.501	23.810	24.347	24.823	24.707	25.462	26.162
Tube with porous media ε = 91% - Nusselt number-											
Re	300	11.705	13.813	13.718	13.824	14.246	14.432	14.645	14.892	15.174	15.496
	500	13.971	16.918	17.036	17.240	17.600	17.924	18.275	18.323	18.809	19.332
	1000	17.657	20.702	20.918	21.152	21.510	21.939	22.399	22.341	22.978	23.659
	1500	21.068	24.183	24.429	24.695	25.113	25.600	26.122	26.069	26.792	27.564

type of nanofluids. The increase in the volume concentration causes the effective viscosity of the nanofluids to rise. The nanoparticles hinder the movement of fluid layers by enhancing momentum exchange, which results in an increase in shear resistance near the tube wall. The Cu/Syltherm 800 nanofluids display the highest friction factor, consistent with their higher conductivity and density and stronger particle-fluid interaction, yet remain viable for thermal system optimization due to their superior heat transfer performance without excessive pressure losses.

8.3.3 Effects of Nanofluids and Semi-Porous Media

The impact of porous media (ε = 0.95) with and without nanofluids on the Nusselt number is depicted in Fig. 7.c. The introduction of nanoparticles clearly leads to an increase in the Nusselt number across all Reynolds numbers and volume fractions. This enhancement is primarily attributed to the improved effective thermal conductivity and intensified microscopic convection resulting from motion and particle–fluid interactions. The improvement is further determined from the data in Table 7, which shows that the best performance was reached with 3% concentration of Cu/Syltherm 800 nanofluid, with the Nusselt number increasing by 15.88% to 29.37% compared to the case of φ = 0% and by 86.09% to 95.63% for the smooth tube.

At the same time, as shown in Fig. 7.d, the friction factor increases due to the higher viscosity and particle concentration. For example, in 8, at φ = 3% and Re = 300, the friction factor for Cu/Syltherm 800 nanofluid reaches 0.254, approximately 1.5 times higher than that of the tube with porous media (ε = 95% in the φ = 3% case) and 7.65 times higher than the smooth tube. However, all values approach closely at higher Reynolds numbers, regardless of the type of nanofluid used or the volume fraction. This variation is due to the dominance of inertial forces over viscous effects; for instance, at Re = 1500 and 3% concentration of Cu/Syltherm 800, the friction factor is about 0.071, which increases by only 1.3 times compared to the φ = 0% case. When the porosity is reduced to ε = 0.91, as shown in Fig. 7.e and supported by the data in Table 7, the Nusselt number rises with the augmenting Reynolds number. Moreover, the incorporation of nanoparticles further enhances convective heat transfer. This improvement is accredited to lower porosity, which increases the number of solid obstacles, promotes more substantial disruption of the flow, and mixes the heat better. In combination with the superior thermal conductivity of nanofluids, particularly Cu/Syltherm 800, a synergistic improvement in heat transfer is observed. At a 3% volume fraction of Cu nanoparticles, the Nusselt number increases by 30.8% to 38.36% compared to the ε = 0.95 case and by up to 128.74% relative to the smooth tube. This nearly 3.5-fold increase highlights the combined effect of intensified solid-fluid interactions and enhanced thermal properties of the nanofluid.

However, this enhancement in heat transfer comes at the expense of an augmented pressure drop. Figure 7.f examines the variation of the friction factor with Reynolds number for a tube containing porous matrices with ε = 0.91. As shown in both Fig. 7.f and Table 8, the friction factor in this configuration is considerably higher than that observed for ε = 0.95 (Fig. 7.d). This increase is primarily due to the denser porous structure, which intensifies fluid–solid interactions and restricts flow passages. For instance, at Re = 1500 and a 3% volume fraction of Cu/Syltherm 800, the friction factor reaches approximately 0.119—about 1.33 times greater than that of the φ = 0% case (same porosity) and significantly higher than the value of 0.071 observed at ε = 0.95 under identical nanofluid conditions. The elevated friction factor is attributed to the reduced flow cross-section and increased surface contact area, both of which enhance viscous dissipation and resistance to flow.

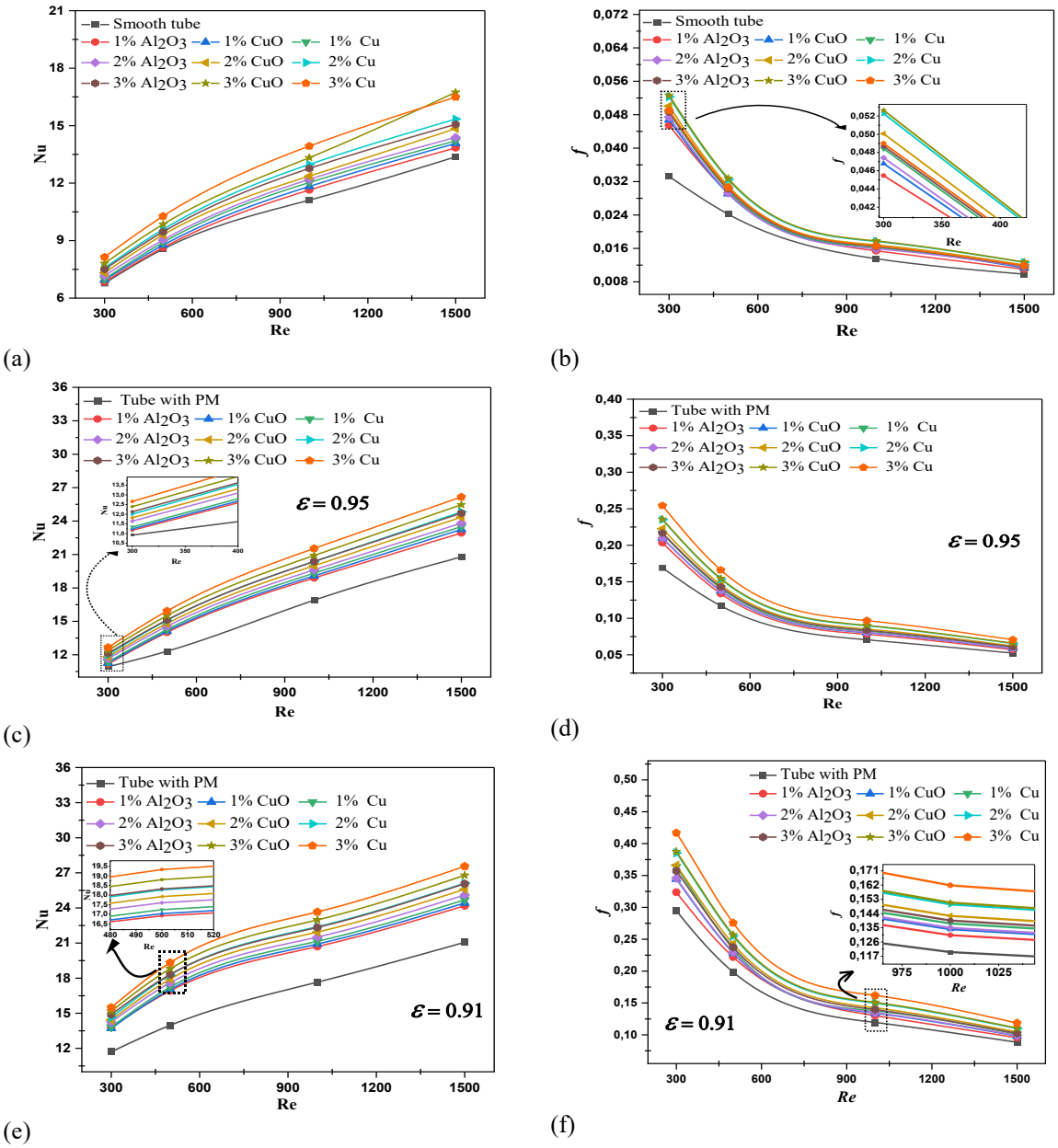

Fig. 7 Nusselt number and friction factor

Table 8 Data of friction factor for a smooth tube, Tube with porous media ε = 95%, and Tube with porous media ε= 91%

Smooth tube-friction factor-											
Volume fraction		0%	1%			2%			3%		
Type of NF		-	Al_2O_3	CuO	Cu	Al_2O_3	CuO	Cu	Al_2O_3	CuO	Cu
Re	300	0.0332	0.0455	0.0468	0.0484	0.0474	0.0501	0.0523	0.0487	0.0526	0.0490
	500	0.0242	0.0294	0.0291	0.0299	0.0293	0.0309	0.0325	0.0303	0.0327	0.0305
	1000	0.0135	0.0154	0.0163	0.0162	0.0159	0.0169	0.0177	0.0165	0.0178	0.0166
	1500	0.0099	0.0110	0.0113	0.0116	0.0117	0.0120	0.0127	0.0118	0.0127	0.0119
Tube with porous media ε = 95% - friction factor-											
Re	300	0.169	0.203	0.210	0.216	0.210	0.223	0.235	0.217	0.236	0.254
	500	0.117	0.134	0.137	0.141	0.138	0.146	0.154	0.143	0.155	0.166
	1000	0.071	0.078	0.080	0.082	0.081	0.085	0.090	0.084	0.090	0.097
	1500	0.052	0.057	0.059	0.060	0.059	0.062	0.065	0.061	0.066	0.071
Tube with porous media ε = 91% - friction factor-											
Re	300	0.295	0.324	0.345	0.364	0.346	0.366	0.386	0.357	0.388	0.417
	500	0.199	0.222	0.228	0.235	0.230	0.243	0.255	0.237	0.257	0.276
	1000	0.120	0.130	0.134	0.138	0.135	0.143	0.150	0.140	0.151	0.162
	1500	0.089	0.096	0.098	0.101	0.099	0.104	0.110	0.102	0.111	0.119

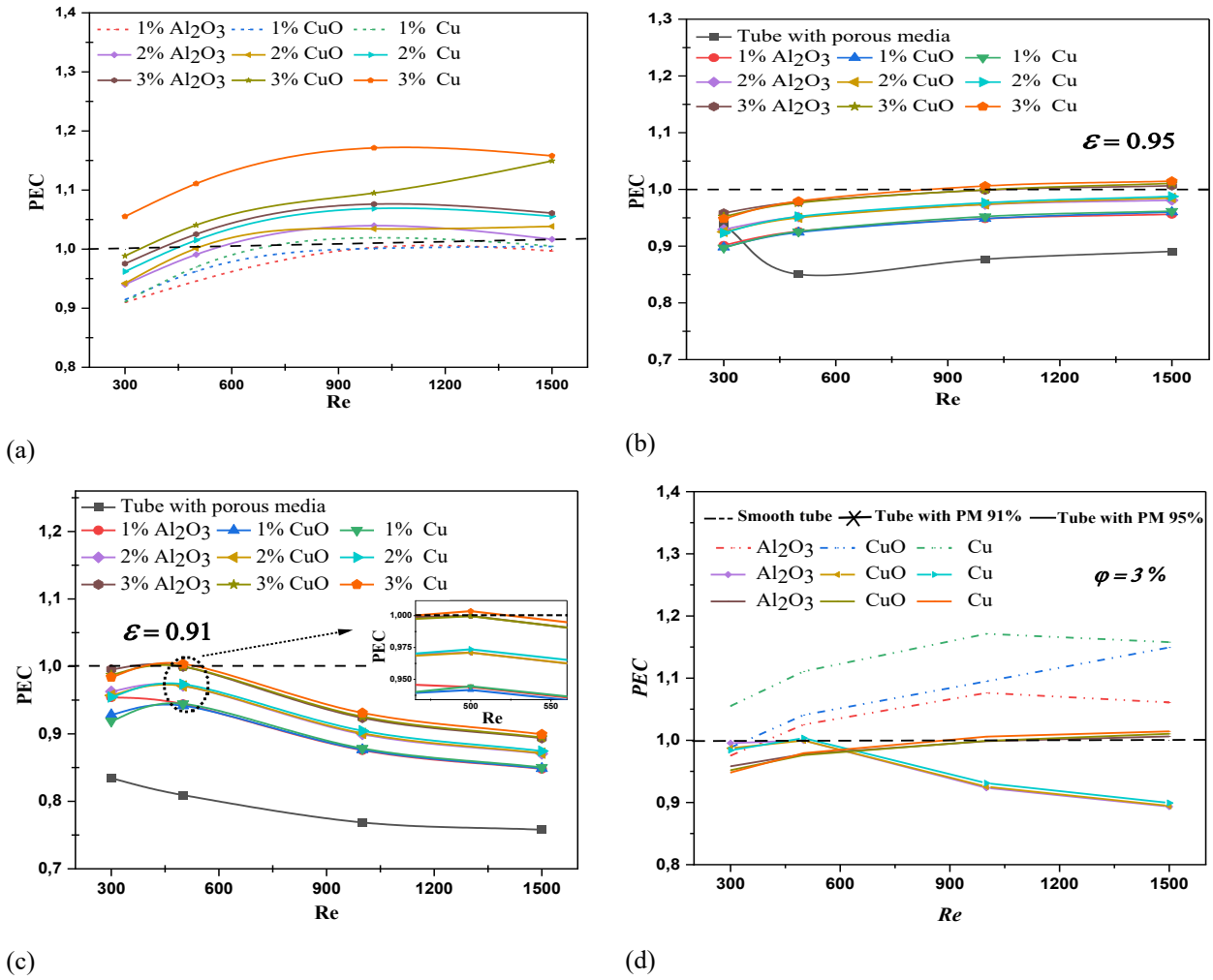

Fig. 8 Performance evaluation criteria for: a) Smooth Tube, b) tube with porous media ε=0.95, c) tube with porous media ε=0.91, and d) different configuration for 3% nanofluid

8.4 The Performance Evaluation Criteria (PEC):

8.4.1 The Effect of Nanofluids without Semi-Porous Media

The performance evaluation criterion, illustrate the balance between the improvement of heat transfer efficiency and pressure drop penalty as summarized in Eq. (12). Figure 8.a shows that the PEC increases with the addition of nanoparticles and with higher volume fractions. The main cause of this trend is the improved thermal conductivity, which significantly enhances heat transfer over the increase in frictional losses. The maximum PEC value of 1.2 is achieved using 3% concentration of Cu/Sylltherm 800 at Reynolds numbers of 1000, wherever thermal performance is predominant, as well as at the higher Reynolds numbers of 1000 and 1500 for all types of nanofluids used.

8.4.2 Effect of Nanofluids and Semi-Porous Media

In Fig. 8.b, for the configuration with a porous medium ε = 95%, the PEC increases when the Reynolds number rises for all types of nanofluids. In addition, at Reynolds number of 300, the performance of the tube with porous media for φ = 0% is better compared to the presence of nanofluid at 1% and 2% volume fractions. This is likely due to the higher viscosity of nanofluids at low flow rates, which increases the pressure drop more than the corresponding heat transfer gain. However, at higher Reynolds numbers (1000 and 1500), the PEC exceeds one for 3% volume fraction for all types of nanofluids used, suggesting that inertial forces dominate, making nanofluids more thermally beneficial. Conversely, when the porosity is reduced to 91% (as shown in Fig.8.c), the PEC generally declines in comparison to the ε = 95% case, indicating that hydraulic performance begins to dominate over thermal performance. Furthermore, when the Reynolds number exceeds 500, the PEC reduces as the Reynolds number increases.

The recapitulation of the three configurations is indicated in Fig. 8.d. The results specify that the addition of a 3% volume fraction of Cu/Sylltherm 800 nanofluid to the smooth tube greatly enhances its performance, thereby yielding the best PEC for all Reynolds numbers. Generally, porous media tubes at 95% porosity showed better performance compared to the ones with 91%, suggesting that: higher porosity increases heat transfer. Adding 3% Cu/sylltherm 800 enhances the PEC in all cases. However, the increased friction factor generated in the tube containing 91% porous media causes a decline in the performance.

8.5 Total Entropy Generation

The impact of nanofluid type, volume fractions, and porous media on total entropy generation in the absorber tube is illustrated in Figs 9.a-d. For the case of a smooth tube (see Fig. 9.a), total entropy generation increases with growing volume fractions. This trend is mainly attributed to the increase in effective viscosity, which enhances viscous dissipation. Also, the insertion of Al_2O_3/Syltherm 800 for different volumes illustrates the lowest entropy generation and has a reduced value compared to the other two cases of nanofluids, indicating lower irreversibilities due to its moderate thermal conductivity and limited impact on flow resistance. Nevertheless, the entropy generation diminishes as the Reynolds number increases. This means enhanced convective heat transfer with a higher Reynolds number and reducing the temperature gradient.

Conversely, as shown in Figs 9b and 9c, the results for novel configurations of tubes with porous media $\varepsilon = 95\%$ and $\varepsilon = 91\%$, respectively, the use of nanofluids together with semi-porous media results in a notable reduction in overall entropy generation. This decrease continues with increasing Reynolds numbers, thereby confirming the improvement in heat transfer efficiency at heightened flow rates. Additionally, the analysis indicates that higher volume fractions lead to a decrease in overall entropy. The most notable reductions occur when the porous medium is combined with Al_2O_3/Syltherm 800, where the entropy values become nearly identical across various volume fractions. In contrast, configurations using porous media alone ($\varphi = 0\%$) display the smallest reduction in overall entropy generation, especially at a high porosity of 91%. This observation highlights the yield of porous media in providing optimal thermal enhancement.

Figure. 9.d shows the entropy generation all configurations proposed with varying Reynolds numbers. The 3% concentration of Cu/Syltherm 800 in smooth tube creates the higher irreversibilities due to both viscous and thermal contributions. The configuration with 91% porosity presents a considerable reduction in entropy generation, engendering improvement in thermal performance and diminution in losses, which confirms the efficacy of solid matrix structures in dissipating entropy and enhancing heat transfer performance under the second law. Adding Cu/Syltherm 800 nanofluid with 3% concentration to porous media doesn't affect entropy production.

8.6 Variation of Bejan number

The variations of the Bejan number with the Reynolds number are illustrated in Figures 9.e–g. In Figure 9.e, corresponding to the smooth tube, it is observed that the Bejan number is only weakly sensitive to the type of nanofluid used (Al_2O_3, CuO, or Cu) for a given volume fraction. This behavior is caused by the relatively minor differences in thermal conductivity and dynamic viscosity between these nanofluids, which results in similar contributions to entropy generation by heat transfer and fluid friction. Therefore, their effect on the Bejan number, which represents the ratio of these two sources of irreversibility, remains minimal. However, increasing the nanoparticle volume fraction causes a noticeable decrease in the Bejan number. This trend can be explained by the increase in nanofluid viscosity at higher concentrations, which enhances the viscous dissipation component of entropy generation. As the dominance of thermal entropy generation diminishes relative to frictional effects, the Bejan number drops accordingly.

The Bejan number decreases even more in Figs 9.f and 9.g compared to the smooth tube. These figures show results for tubes filled with porous media of porosity 0.95 and 0.91, respectively. At lower porosities, this reduction becomes more pronounced. Increased flow resistance and viscous effects brought on by the porous medium enhance the generation of entropy as a result of fluid friction. Consequently, heat transfer no longer dominates the total irreversibility, lowering the Bejan number. This behavior is heightened by the use of nanofluids in conjunction with porous media, especially at high Reynolds numbers where viscous losses become more noticeable.

Figure 9.h summarizes the variations of the Bejan number with the number of Reynolds in three configurations studied, specifically for 3% Cu/Syltherm 800, which gave us the highest performance. The Be value is close to 1 for all cases at small Reynolds numbers. The heat transfer irreversibility is more dominant than the friction one. The Bejan number diminishes whenever the Reynolds number increases in all cases. Tubes incorporating porous media have a minimum Be number value, especially at 91% porosity, revealing the influence of the flow resistance.

8.7 Summarizing

The performance evaluation criterion (PEC) and entropy production ($S^{'}_{gen}$) provide important information for improving heat transfer and thermodynamic efficiency in the receiver of a parabolic trough collector, as shown in Fig. 10.

The combined analysis reveals the trade-off between PEC and entropy generation, with 3% Cu exhibiting high performance in three different configurations: a smooth tube, a tube with a semi-porous medium insert, and two different porosities (91% and 95%). We select Re = 1000 as an example.

The performance evaluation criterion in Figure 10.a shows high thermal efficiency in a smooth tube with nanofluids. However, this parameter decreases when inserting a porous medium alone, but they rise again when the porous medium is combined with nanofluid, as shown in Figure 10.b.

Cu nanoparticles are the most thermally efficient when combined with Syltherm 800, providing high performance at a 3% concentration, especially for Re = 1000, as shown in Figure 10b.

The entropy generation shown in Figure 10.c indicates that the smooth tube generates the most entropy. Nevertheless, the tubes with porosities ($\varepsilon = 95\%$ and $\varepsilon = 91\%$) exhibit decreased entropy production, indicating enhanced energy efficiency, as shown in Figure 10.d.

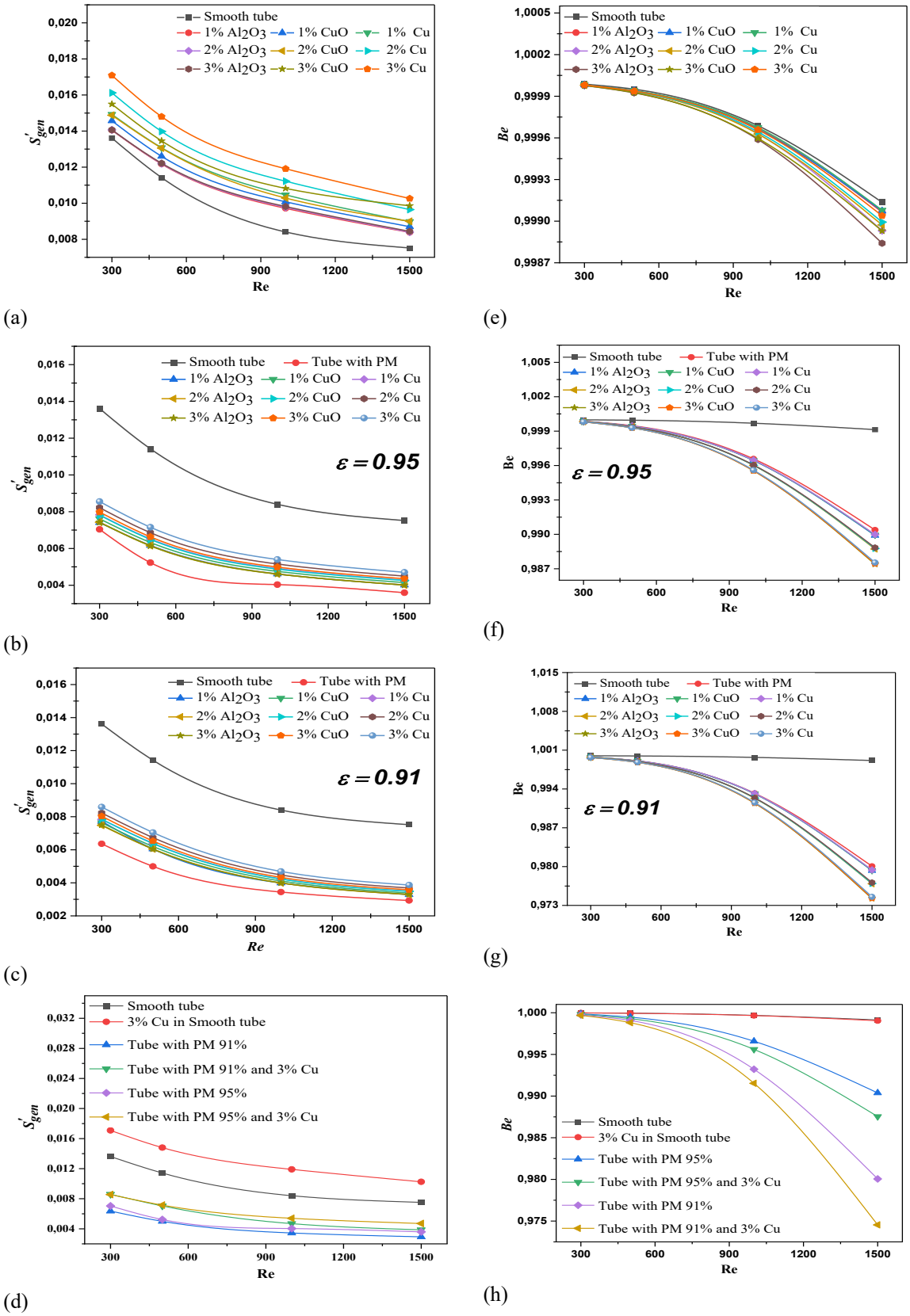

Fig. 9 Total Entropy generation and Bejan number.

9. CONCLUSION AND FUTURE WORK

In this work, the impact of square porous media introduced as seven matrices with varying porosities (95% and 91%) in the receiver tube of a parabolic trough collector is examined numerically. Three mono-nanofluid types (Al_2O_3/Syltherm 800, CuO/Syltherm 800, and Cu/Syltherm 800) are studied at three volume fractions (1%, 2%, and 3%), which are used as working fluids. This paper presents a comparison between the two study cases: porous medium and nanofluid combined. The results indicate the following:

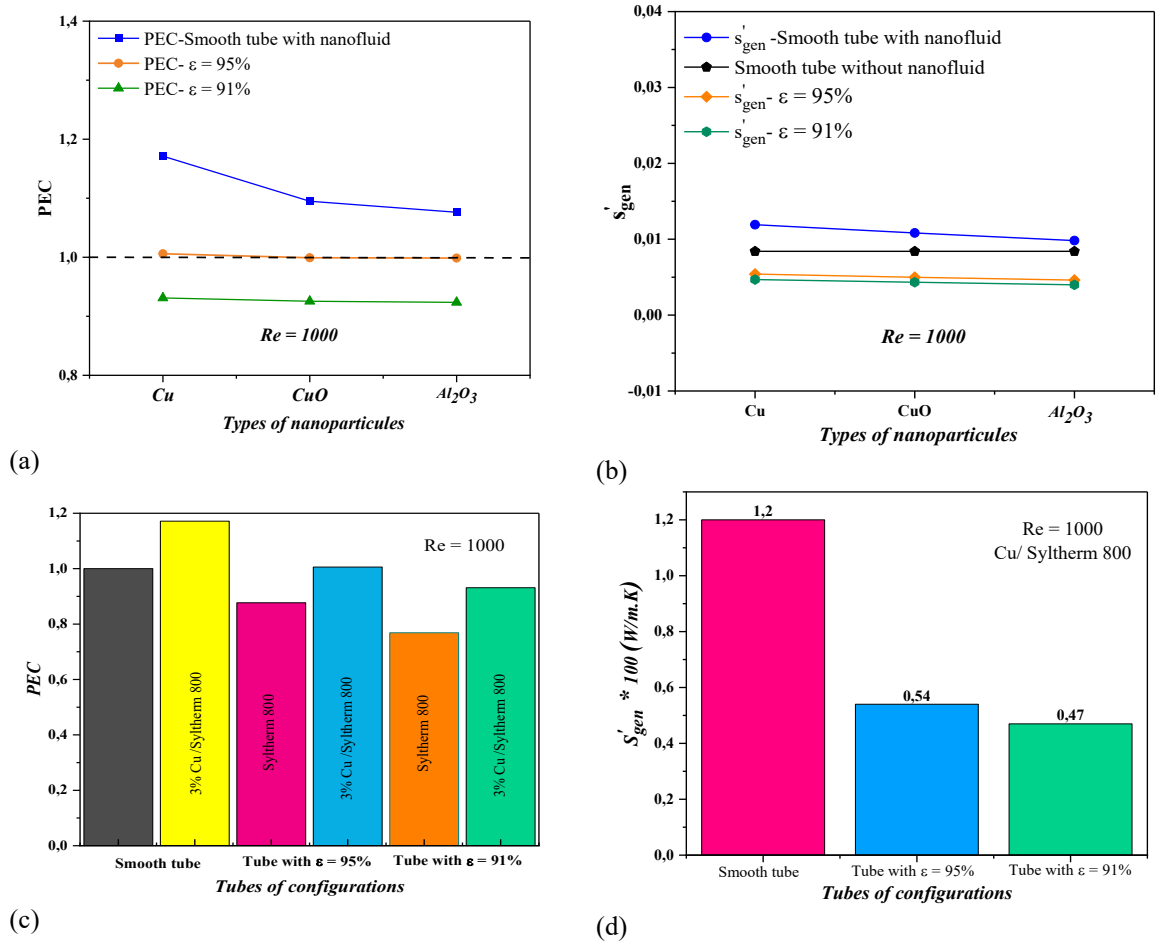

Fig. 10 Summarize the Performance evaluation criteria and Entropy generation for Re =1000

- The presence of nanofluids significantly enhanced the Nusselt number, especially at a 3% concentration of using Cu/Syltherm 800 nanofluids.
- The combination of porous medium and nanofluids works together to improve heat transfer by the nanofluid and distribute heat concentration by the porous medium.
- Reducing porosity from 95% to 91% in the novel configurations enhanced heat transfer and improved thermal homogeneousness, but it also increased the coefficient of friction (pressure drop) due to increased resistance to flow.
- The configuration with ε = 95% porosity suggests a good balance between heat transfer enhancement and moderate pressure drop, making them a thermally efficient option without excessive energy loss.
- A smooth tube with a 3% concentration of Cu/Syltherm 800 nanofluid gave the best PEC, while a porous media with ε = 95% porosity provided a good balance between improving heat transfer and moderating the pressure compared to ε = 91%.
- The novel configurations with porous media reduce the PEC compared to smooth tubes with nanofluid. Still, it regulates the temperature and heat homogeneity inside the tube receiver, which are the most essential goals in PTC configurations.
- The smooth tubes with nanofluids achieved the highest thermal enhancement; however, they also resulted in higher entropy generation, indicating higher thermal losses. This may limit their viability as long-term sustainable solutions.
- The novel tube reduces thermal energy losses by minimizing entropy generation, which makes the system more sustainable for long-term thermal applications.
- The Bejan number is unaffected by the type of nanofluid; however, it is visibly decreased when the volume fraction is combined with porous media.

This work contributes to improving the performance and sustainability of parabolic trough solar collectors (PTCs) by optimizing the receiver design, incorporating nanofluids, and integrating porous media. These simulated designs allowed the heat transfer to enhance, helped with temperature uniformity, and reduced entropy generation. The novelty configuration can effectively extend the lifespan and also reduce the operational costs of the absorber tube. The optimal design of the proposed PTC receiver can increase energy efficiency, making solar thermal technology more competitive and financially viable for large-scale applications.

The future work focuses on constructing real PTC prototypes and experimentally validating the numerical findings under realistic operating conditions. Practical

challenges that need to be addressed are increased pressure drop, long-term nanofluid stability, and material durability in concentrated solar flux. These efforts aim to further optimization of receiver performance and improve system durability by minimizing thermal stresses. Also, it is possible to combine it with phase change materials (PCMs) to get the best of both worlds: better thermal performance and thermal energy storage. By combining porous media with advanced nanofluids, the method could also be used with other solar systems, like PV/T collectors. This combination would lead to solar thermal technologies that are more efficient, competitive, and long-lasting.

CONFLICT OF INTEREST

The corresponding author confirms that there are no conflicts of interest for the entire team of authors.

AUTHORS CONTRIBUTION

H. Diafi: Software, Writing original draft, Investigation, Visualization, Formal analysis, data curation. **S. Djouimaa:** Project administration, Supervision, Writing – review, Methodology. **D. Guerraiche:** Data curation, Writing – review, formal analysis, supervision, Visualization. **S. Noui:** validation, review- editing, resources.

REFERENCES

Abbasi, H. R., Sharifi Sedeh, E., Pourrahmani, H., & Mohammadi, M. H. (2020). Shape optimization of segmental porous baffles for enhanced thermo-hydraulic performance of shell-and-tube heat exchanger. *Applied Thermal Engineering*, *180*(July). https://doi.org/10.1016/j.applthermaleng.2020.115835

Bejan, A. (1996). Entropy generation minimization: The new thermodynamics of finite-size devices and finite-time processes. *Journal of Applied Physics*, *79*(3), 1191–1218. https://doi.org/10.1063/1.362674

Bozorg, M. V., Hossein Doranehgard, M., Hong, K., & Xiong, Q. (2020). CFD study of heat transfer and fluid flow in a parabolic trough solar receiver with internal annular porous structure and synthetic oil–Al2O3 nanofluid. *Renewable Energy*, *145*, 2598–2614. https://doi.org/10.1016/j.renene.2019.08.042

Brinkman, H. C. (1952). The viscosity of concentrated suspensions and solutions. *The Journal of Chemical Physics*, *20*(4), 571. https://doi.org/10.1063/1.1700493

Büyük Öğüt, E. (2009). Natural convection of water-based nanofluids in an inclined enclosure with a heat source. *International Journal of Thermal Sciences*, *48*(11), 2063–2073. https://doi.org/10.1016/j.ijthermalsci.2009.03.014

Chakraborty, O., & Nath, S. (2024a). Optimizing the thermal performance in parabolic solar trough collectors: investigating the impact of ionic nanofluid and revolving fins inserts. *Clean Technologies and Environmental Policy*. https://doi.org/10.1007/s10098-024-03076-7

Chakraborty, O., & Nath, S. (2024b). Thermal performance simulation of parabolic trough collector with ternary nanofluid flows and half-star-shaped fins inserts in different receivers. *Journal of the Brazilian Society of Mechanical Sciences and Engineering*, *46*(3), 114. https://doi.org/10.1007/s40430-024-04680-w

Chen, X., Xia, X. L., Liu, H., Li, Y., & Liu, B. (2016). Heat transfer analysis of a volumetric solar receiver by coupling the solar radiation transport and internal heat transfer. *Energy Conversion and Management*, *114*, 20–27. https://doi.org/10.1016/j.enconman.2016.01.074

Das, S., Verma, N., Pathak, M., & Bhattacharyya, S. (2021). Axially oriented structured porous layers for heat transfer enhancement in a solar receiver tube. *Journal of Thermal Science*, *30*(5), 1643–1657. https://doi.org/10.1007/s11630-021-1514-4

Delgado-Torres, A. M., & García-Rodríguez, L. (2007). Comparison of solar technologies for driving a desalination system by means of an organic Rankine cycle. *Desalination*, *216*(1–3), 276–291. https://doi.org/10.1016/j.desal.2006.12.013

Ekiciler, R., Arslan, K., & Turgut, O. (2023). Application of nanofluid flow in entropy generation and thermal performance analysis of parabolic trough solar collector: experimental and numerical study. *Journal of Thermal Analysis and Calorimetry*, *148*(14), 7299–7318. https://doi.org/10.1007/s10973-023-12187-0,

Esapour, M., Hamzehnezhad, A., Rabienataj Darzi, A. A., & Jourabian, M. (2018). Melting and solidification of PCM embedded in porous metal foam in horizontal multi-tube heat storage system. *Energy Conversion and Management*, *171*(January), 398–410. https://doi.org/10.1016/j.enconman.2018.05.086

Esmaeili, Z., Valipour, M. S., Rashidi, S., & Akbarzadeh, S. (2023). Performance analysis of a parabolic trough collector using partial metal foam inside an absorber tube: an experimental study. *Environmental Science and Pollution Research*, *30*(38), 89794–89804. https://doi.org/10.1007/s11356-023-28732-1

Guerraiche, D., Guerraiche, K., Driss, Z., Chibani, A., Merouani, S., & Bougriou, C. (2022). Heat Transfer Enhancement in a Receiver Tube of Solar Collector Using Various Materials and Nanofluids. *Engineering, Technology and Applied Science Research*, *12*(5), 9282–9294. https://doi.org/10.48084/etasr.5214

Hatami, M., Geng, J., & Jing, D. (2018). Enhanced efficiency in Concentrated Parabolic Solar Collector (CPSC) with a porous absorber tube filled with

metal nanoparticle suspension. *Green Energy and Environment*, *3*(2), 129–137. https://doi.org/10.1016/j.gee.2017.12.002

Heyhat, M. M., Valizade, M., Abdolahzade, S., & Maerefat, M. (2020). Thermal efficiency enhancement of direct absorption parabolic trough solar collector (DAPTSC) by using nanofluid and metal foam. *Energy*, *192*. https://doi.org/10.1016/j.energy.2019.116662

Hooshmand, A., Zahmatkesh, I., Karami, M., & Delfani, S. (2021). Exergy analysis of a nanofluid – based direct absorption solar collector (DASC) Occupied by Porous Foam. *Challenges in Nano and Micro Scale Science and Technology, 9*(1), 1–11. https://doi.org/10.22111/CNMST.2021.38759.1212

Jamal-Abad, M. T., Saedodin, S., & Aminy, M. (2017). Experimental investigation on a solar parabolic trough collector for absorber tube filled with porous media. *Renewable Energy*, *107*, 156–163. https://doi.org/10.1016/j.renene.2017.02.004

Jamal-Abad, M. T., Saedodin, S., & Aminy, M. (2018). Variable conductivity in forced convection for a tube filled with porous media: A perturbation solution. *Ain Shams Engineering Journal*, *9*(4), 689–696. https://doi.org/10.1016/j.asej.2016.03.019

Kuwahara, F., Shirota, M., & Nakayama, A. (2001a). A numerical study of interfacial convective heat transfer coefficient in two-energy equation model of porous media. *International Journal of Heat and Mass Transfer*, *44*(6), 1153–1159. https://doi.org/10.1299/kikaib.66.1430

Kuwahara, F., Shirota, M., & Nakayama, A. (2001b). A numerical study of interfacial convective heat transfer coefficient in two-energy equation model of porous media. *International Journal of Heat and Mass Transfer*, *44*(6), 1153–1159. https://doi.org/10.1299/kikaib.66.1430

Maxwell, J. C. (1881). *A treatise on electricity and magnetism*. Oxford: Clarendon Press.

Mwesigye, A., Bello-Ochende, T., & Meyer, J. P. (2013). Numerical investigation of entropy generation in a parabolic trough receiver at different concentration ratios. *Energy*, *53*, 114–127. https://doi.org/10.1016/j.energy.2013.03.006

Naaim, S., Ouhammou, B., El Merabet, Y., Aggour, M., Mihi, M., El Mers, E. M., & Daouchi, B. (2025). Optimization of nanoparticle concentration for enhanced performance of Therminol® VP-1-based nanofluids in parabolic trough systems. *Results in Engineering*, *26*. https://doi.org/10.1016/j.rineng.2025.105051

Pak, B. C., & Cho, Y. I. (1998). Hydrodynamic and heat transfer study of dispersed fluids with submicron metallic oxide particles. *Experimental Heat Transfer*, *11*(2), 151–170. https://doi.org/10.1080/08916159808946559

Panja, S. K., Das, B., & Mahesh, V. (2024). Numerical study of parabolic trough solar collector's thermo-hydraulic performance using CuO and Al2O3 nanofluids. *Applied Thermal Engineering*, *248*, 123179. https://doi.org/10.1016/j.applthermaleng.2024.123179

Peng, H., Li, M., & Liang, X. (2020). Thermal-hydraulic and thermodynamic performance of parabolic trough solar receiver partially filled with gradient metal foam. *Energy*, *211*. https://doi.org/10.1016/j.energy.2020.119046

Peng, H., Li, M., Hu, F., & Feng, S. (2021). Performance analysis of absorber tube in parabolic trough solar collector inserted with semi-annular and fin shape metal foam hybrid structure. *Case Studies in Thermal Engineering*, *26*(April), 101112. https://doi.org/10.1016/j.csite.2021.101112

Ravi Kumar, K., & Reddy, K. S. (2012). Effect of porous disc receiver configurations on performance of solar parabolic trough concentrator. *Heat and Mass Transfer/Waerme- Und Stoffuebertragung*, *48*(3), 555–571. https://doi.org/10.1007/s00231-011-0903-8

Shah, R. K., & London, A. L. (1978). *Laminar flow forced convection in ducts: a source book for compact heat exchanger analytical data.* Laminar Flow Forced Convection in Ducts: Vol. Suppl. 1.

Sheikholeslami, M., & Khalili, Z. (2025). Simulation of a photovoltaic panel with a novel cooling duct using ternary nanofluid and integrated with a thermoelectric generator. *Journal of the Taiwan Institute of Chemical Engineers*, *170*, 105982. https://doi.org/https://doi.org/10.1016/j.jtice.2025.105982

Sheikholeslami, M., Khalili, Z., Salehi, F. & Momayez, L. (2025). Simulation of sustainable solar thermal storage system involving photovoltaic panel equipped with nanofluid-based splitter considering self-cleaning coating. *Sustainable Cities and Society*, *119*, 106100. https://doi.org/https://doi.org/10.1016/j.scs.2024.106100

Tayebi, R., Akbarzadeh, S., & Valipour, M. S. (2019). Numerical investigation of efficiency enhancement in a direct absorption parabolic trough collector occupied by a porous medium and saturated by a nanofluid. *Environmental Progress and Sustainable Energy*, *38*(2), 727–740. https://doi.org/10.1002/ep.13010

Tayebi, T., & Chamkha, A. J. (2016). Numerical Heat Transfer, Part A: Applications Free convection enhancement in an annulus between horizontal confocal elliptical cylinders using hybrid nanofluids. *Numerical Heat Transfer, Part A: Applications*, *0*(0), 1–16. https://doi.org/10.1080/10407782.2016.1230423

Valizade, M., Heyhat, M. M., & Maerefat, M. (2020). Experimental study of the thermal behavior of direct absorption parabolic trough collector by applying copper metal foam as volumetric solar absorption. *Renewable Energy*, *145*, 261–269. https://doi.org/10.1016/j.renene.2019.05.112

Wakao, N., & Kagei, S. (1982). *Heat and Mass Transfer in Packed Beds*. Gordon and Breach Science Publishers.

Wang, P., Liu, D. Y., & Xu, C. (2013). Numerical study of heat transfer enhancement in the receiver tube of direct steam generation with parabolic trough by inserting metal foams. *Applied Energy*, *102*, 449–460. https://doi.org/10.1016/j.apenergy.2012.07.026

Webb, R. L. (1981). Performance evaluation criteria for use of enhanced heat trensfer surfaces in heat exhanger design. *International Journal of Heat and Mass Transfer,* 24 (4). https://doi.org/10.1016/0017-9310(81)90015-6

Wei, Y. K., Zhang, J. D., Cheng, Z. D., Gao, Q. P., & He, Y. L. (2024). Numerical study on novel parabolic trough solar receiver-reactors with double-channel structure catalyst particle packed beds by developing actual three-dimensional catalyst porosity distributions. *Chemical Engineering Science*, *287*(January), 119693. https://doi.org/10.1016/j.ces.2023.119693

Xu, C., Song, Z., Chen, L. der., & Zhen, Y. (2011). Numerical investigation on porous media heat transfer in a solar tower receiver. *Renewable Energy*, *36*(3), 1138–1144. https://doi.org/10.1016/j.renene.2010.09.017